large single crystals; polycrystalline arrays may be brittle. Such composites may be of use as high-performance damping materials, since the figure of merit[26] in the present results exceeds that of commonly used materials ($E\tan\delta \approx 0.6$ GPa) by a factor of more than 20. For that purpose, sensitivity to temperature could be reduced via matching inclusion and matrix stiffness. Moreover, pre-stressed or pre-buckled[24] elements with minimal temperature sensitivity may be used as inclusions. Bounds on properties of complex heterogeneous materials are generally derived assuming positive phase properties[18]. These bounds can be exceeded if negative stiffness is allowed, permitting extreme properties not previously anticipated. As in thermoelastic and piezoelectric materials, elasticity is coupled with temperature and electric field respectively, these composites may find use in high-performance sensors and actuators. These composites may also occur naturally in rocks and in biological materials (in which anomalies were reported[27]); they may be considered in the context of deep-focus earthquakes and attenuation of seismic waves. □

Received 25 July 2000; accepted 2 February 2001.

1. Timoshenko, S. P. & Goodier, J. N. *Theory of Elasticity* 3rd edn (McGraw-Hill, New York, 1970).
2. Lakes, R. S. Foam structures with a negative Poisson's ratio. *Science* **235,** 1038–1040 (1987).
3. Lakes, R. S. Advances in negative Poisson's ratio materials. *Adv. Mater.* **5,** 293–296 (1993).
4. Haeri, A. Y., Weidner, D. J. & Parise, J. B. Elasticity of α-cristobalite: a silicon dioxide with a negative Poisson's ratio. *Science* **257,** 650–652 (1992).
5. Rothenburg, L., Berlin, A. A. & Bathurst, R. J. Microstructure of isotropic materials with negative Poisson's ratio. *Nature* **354,** 470–472 (1991).
6. Baughman, R. H., Shacklette, J. M., Zakhidov, A. A. & Stafstrom, S. Negative Poisson's ratios as a common feature of cubic metals. *Nature* **392,** 362–365 (1998).
7. Thompson, J. M. T. Stability prediction through a succession of folds. *Phil. Trans. R. Soc. Lond.* **292,** 1–23 (1979).
8. Thompson, J. M. T. 'Paradoxical' mechanics under fluid flow. *Nature* **296,** 135–137 (1982).
9. Lakes, R. S. & Drugan, W. J. Stiff elastic composite materials with a negative stiffness phase. *J. Mech. Phys. Solids* (submitted).
10. Heckingbottom, R. & Linnett, J. W. Structure of vanadium dioxide. *Nature* **194,** 678 (1962).
11. Paquet, D. & Leroux-Hagon, P. Electron correlations and electron-lattice interactions in the metal-insulator ferroelastic transition in VO_2: a thermodynamical study. *Phys. Rev. B* **22,** 5284–5301 (1979).
12. Zhang, J. X., Yang, Z. H. & Fung, P. C. W. Dissipation function of the first-order phase transformation in VO_2 ceramics by internal friction measurements. *Phys. Rev. B* **52,** 278–284 (1995).
13. *Handbook of Chemistry and Physics* C-40 12–40 (CRC Press, Boca Raton, Florida, 1996).
14. Brodt, M., Cook, L. S. & Lakes, R. S. Apparatus for measuring viscoelastic properties over ten decades: refinements. *Rev. Sci. Instrum.* **66,** 5292–5297 (1995).
15. Lakes, R. S. & Quackenbush, J. Viscoelastic behaviour in indium tin alloys over a wide range of frequency and time. *Phil. Mag. Lett.* **74,** 227–232 (1996).
16. Bramble, J. H. & Payne, L. E. On the uniqueness problem in the second boundary value problem in elasticity. *Proc. 4th Natl Cong. Appl. Mech.* 469–473 (American Society of Mechanical Engineers, Berkeley, California, 1963).
17. Knowles, J. K. & Sternberg, E. On the failure of ellipticity and the emergence of discontinuous gradients in plane finite elastostatics. *J. Elasticity* **8,** 329–379 (1978).
18. Hashin, Z. & Shtrikman, S. A variational approach to the theory of the elastic behavior of multiphase materials. *J. Mech. Phys. Solids* **11,** 127–140 (1963).
19. Read, W. T. Stress analysis for compressible viscoelastic materials. *J. Appl. Phys.* **21,** 671–674 (1950).
20. Hashin, Z. Viscoelastic behavior of heterogeneous media. *J. Appl. Mech. Trans. ASME* **32E,** 630–636 (1965).
21. Lakes, R. S. Extreme damping in composite materials with a negative stiffness phase. *Phys. Rev. Lett.* (in the press).
22. Rosakis, P., Ruina, A. & Lakes, R. S. Microbuckling instability in elastomeric cellular solids. *J. Mater. Sci.* **28,** 4667–4672 (1993).
23. Salje, E. *Phase Transitions in Ferroelastic and Co-elastic Crystals* 10, 72 (Cambridge Univ. Press, Cambridge, 1990).
24. Lakes, R. S. Extreme damping in compliant composites with a negative stiffness phase. *Phil. Mag. Lett.* **81,** 95–100 (2001).
25. Ren, X. & Otsuka, K. Origin of rubber-like behaviour in metal alloys. *Nature* **389,** 579–583 (1997).
26. Cremer, L., Heckl, M. A. & Ungar, E. E. *Structure Borne Sound* 2nd edn 243–247 (Springer, Berlin, 1988).
27. Pugh, J. W., Rose, R. M., Paul, I. L. & Radin, E. L. Mechanical resonance spectra in human cancellous bone. *Science* **181,** 271–272 (1973).
28. Falk, F. Model free energy, mechanics, and thermodynamics of shape memory alloys. *Acta Metall.* **28,** 1773–1780 (1980).
29. Duffy, W. Acoustic quality factor of aluminum alloys from 50 mK to 300 K. *J. Appl. Phys.* **68,** 5601–5609 (1990).

Acknowledgements

We thank W. Drugan and R. Cooper for supportive comments and discussions. This work was supported by the NSF.

Correspondence and requests for materials should be addressed to R.S.L. (e-mail: lakes@engr.wisc.edu).

Climate variability 50,000 years ago in mid-latitude Chile as reconstructed from tree rings

Fidel A. Roig*, Carlos Le-Quesne†‡, José A. Boninsegna*, Keith R. Briffa§, Antonio Lara‡, Håkan Grudd‖, Philip D. Jones§ & Carolina Villagrán¶

* *Laboratorio de Dendrocronología, IANIGLA-CONICET, CC 330 (5500) Mendoza, Argentina*
† *Department Botánica, Facultad de Biología, Universidad de Oviedo, Catedrático Rodrigo Uría s/n, 33006, Spain*
‡ *Instituto de Silvicultura, Universidad Austral de Valdivia, Casilla 567, Valdivia, Chile*
§ *Climate Research Unit, School of Environmental Sciences, University of East Anglia, Norwich NR4 7TJ, UK*
‖ *Department of Physical Geography, Stockholm University, S-10691 Stockholm, Sweden*
¶ *Department Biología, Facultad de Ciencias, Universidad de Chile, Casilla 653, Santiago, Chile*

High-resolution proxies of past climate are essential for a better understanding of the climate system[1]. Tree rings are routinely used to reconstruct Holocene climate variations at high temporal resolution[2], but only rarely have they offered insight into climate variability during earlier periods[3]. *Fitzroya cupressoides*—a South American conifer which attains ages up to 3,600 years—has been shown to record summer temperatures in northern Patagonia during the past few millennia[4]. Here we report a floating 1,229-year chronology developed from subfossil stumps of *F. cupressoides* in southern Chile that dates back to approximately 50,000 ^{14}C years before present. We use this chronology to calculate the spectral characteristics of climate variability in this time, which was probably an interstadial (relatively warm) period. Growth oscillations at periods of 150–250, 87–94, 45.5, 24.1, 17.8, 9.3 and 2.7–5.3 years are identified in the annual subfossil record. A comparison with the power spectra of chronologies derived from living *F. cupressoides* trees shows strong similarities with the 50,000-year-old chronology, indicating that similar growth forcing factors operated in this glacial interstadial phase as in the current interglacial conditions.

With the exception of polar and tropical ice cores and some ocean-sediment cores, palaeoclimate records with annual resolution based on studies of tree rings, coral, and varved sediments have been recovered only for the late Holocene[5]. Here we report annually resolved proxies of palaeoclimate data for southern South America for an interstadial period thought to correspond to marine oxygen isotope stage 3 (OIS 3; ref. 6). Our analysis is based on subfossil tree remnants found at Seno Reloncaví in the southern Lake District of Chile (40° 00′ to 42° 30′ S, 71° 30′ to 74° 00′ W). Here we use the term 'subfossil' to mean wood preserved since the late Pleistocene epoch that still contains carbon material. Supported by glacial geology and palynology studies, the southern Lake District represents an area where late Quaternary climate fluctuations have been best established for the entire Andes[7–10]. Although the Lake District was affected repeatedly by large ice lobes descending from the Andes at times > 14 kyr before present (BP), long-term full-glacial stratigraphic pollen records show that the forests did not completely disappear during the periods of ice advance and rapidly re-expanded afterwards[8,9]. After ice recession, evergreen forest, mainly dominated by broad-leaved and conifer elements, expanded across the Lake District with a wide ecological amplitude, from lowland floodplains to near the modern, upper tree line.

Annually resolved records in the region based on the characteristic

© 2001 Macmillan Magazines Ltd

tree of the north Patagonian evergreen forest, *F. cupressoides* (alerce)—which attains ages of 3,600 years[11]—were available previously only for the past few millennia. *Fitzroya*, a monotypic conifer restricted to wet environments, is a sensitive indicator of climate; both the width and the density of the annual rings respond primarily to variations of summer (December to March) temperatures[11–13]. In southern Chile, present seasonal climates are regulated by the annual cycle of latitudinal migration of the South Pacific Subtropical High coupled with the cold off-shore Humboldt ocean current and the orographic effects of the Andes[14]. The prevailing westerly storm tracks are related to equatorward shifts of the polar front. These low-pressure storms, which are most frequent during winter, are responsible for the humid and equable climate that supports the temperate rain forests.

In the forested landscape of southern Chile and Argentina, acidic soils and climate are conducive to the preservation of tree remnants suitable for radiocarbon dating and dendrochronological research[6,15]. After the 1960 earthquake[16] that affected the southern Lake District, an intertidal area alongside the north shore of Seno Reloncaví became subject to marine erosion. Well preserved subfossil *F. cupressoides* stumps were exposed; the trees had been originally buried *in situ* by a lahar[17] (a debris flow composed chiefly of volcaniclastic materials). Particularly at the Pelluco site (6 km east of Puerto Montt, 41.5° S, 72.9° W), these stumps attain diameters of up to 1–1.5 m. Few stumps recovered from Pelluco belong to *Pilgerodendron uviferum*. This is evocative of the present-day *Fitzroya–Pilgerodendron* community on marshy, low-drainage soils[13]. Because the outermost rings have been eroded from most of the cross-sections, it was impossible to ascertain if the trees were killed and buried simultaneously in sediment. However, the position and orientation of the stumps suggest that this forest was affected by a catastrophic single event. Tephra deposition, flooding and abrupt changes of the ground level—caused, for example, by earthquakes—today affect the stability of *F. cupressoides* forests[18]; these factors must have operated similarly in the past.

The AMS (accelerator mass spectrometry) ^{14}C ages of three wood samples containing the five innermost rings are 49,780 ± 2,040 ^{14}C yr BP, 49,770 ± 2,040 ^{14}C yr BP, and 49,370 ± 2,000 ^{14}C yr BP (CAMS 46534, 46535, and 46536 respectively). Previous radiocarbon dating showed similar results[17,19]. Because these dates are close to or higher than the limit for ^{14}C dating, they should be regarded as minimum ages for the subfossil wood. According to the chronological and stratigraphic glacial record proposed for the area[7], the wood samples pre-date the Last Glacial Maximum, and broadly correspond to the early portions of middle Llanquihue time (correlated with the Middle Wisconsinan/Weichselian glacial stages in the Northern Hemisphere). Furthermore, the longer pollen records available for the region[8,9] document the existence of an arboreal taxa association with a significant presence of *Fitzroya*-related pollen types (*Pilgerodendron* type) in the early phases of middle Llanquihue time (that is, about 47,000 ^{14}C yr BP). This implies that tracts of interstadial forest immediately adapted to growth under the cool temperate, humid, climate regime in the mid-latitudes of southern Chile at the early stages of OIS 3. The simplest explanation, pending more precise dates, is that the subfossil *Fitzroya* stand became established during an interval of humid and cool climate, broadly corresponding to the onset of OIS 3.

Subfossil wood samples from Pelluco were collected by different workers from Chile, Sweden and Argentina, and processed according to standard dendrochronological techniques[20]. 51 polished transverse cross-sectional surfaces from 30 trees were measured (with a precision of ± 0.01 mm), and the resulting individual ring-width series were subjected to extensive cross-dating comparisons to identify missing rings and eliminate other possible errors at the measuring stage. After this procedure, 47 radii from 28 trees were selected and used to construct a floating mean tree-ring chronology 1,229 years long (the range of specimen length was 185–1,154 years). Tree-ring standardization[20] was performed to remove the inherent long-term growth trend associated with tree age and forest dynamics. Individual series were detrended using a smoothing spline with a fixed 50% frequency response of 200 years, resulting in dimensionless indices, before averaging them into the chronology. This standardization procedure preserves most of the century-timescale tree growth variations[21]. The final chronology, with the corresponding internal sample replication, is shown in Fig. 1. To our knowledge, this is the oldest known floating (that is, not absolutely dated) tree-ring chronology developed to date.

To identify cycles contained in our Pelluco chronology, spectral analysis was performed using two different methods as defined in Fig. 2. Fourier analysis (using the Blackman-Tukey technique) showed that long-term cyclic components exceeding the *a priori*

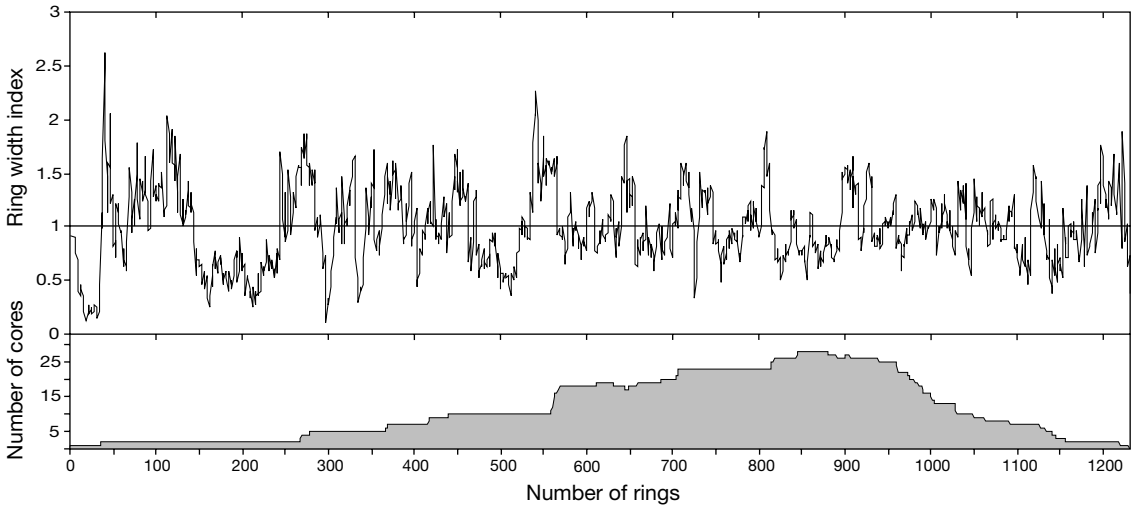

Figure 1 The 1,229-year-long floating tree-ring chronology from Pelluco, southern Chile. A cross-dated set of 47 ring-width radii obtained from 28 subfossil trees make up the ARSTAN (AutoRegressive STANdardization) chronology, whose best replicated section (more than 5 series) exists between relative rings 278 and 1,139. The subfossil chronology shows notable year-by-year changes in ring widths. Those periods with very narrow rings (two cells wide) make measurement and cross-dating rather difficult. Missing rings were infrequent. The overall series mean ring-width is 0.42 mm and the cross-correlation average between all series is 0.53, with a mean series length of 430 years. The signal-to-noise ratio is relatively high at 5.25, and the variance explained by the first eigenvector is 32.27%. The first-order autocorrelation is 0.85 and the mean sensitivity is 0.15. These values are similar to the statistics of living *Fitzroya* chronologies[4,27].

© 2001 Macmillan Magazines Ltd

95% significance level occur at periods of 153–245 and 87–94 years, which respectively account for 21.38% and 19.71% of the variance in the power spectrum. Other significant peaks in the spectrum, which account for the 13% of total variance, fall within the higher frequency band (periodicities in the range of 2–7 years; Fig. 2a inset). The same cycles are reproduced in the maximum entropy power spectrum (not shown here).

The Blackman-Tukey and maximum-entropy spectral properties of the chronologies derived from living *Fitzroya* trees are broadly similar to those identified in the subfossil series (that is, the peaks at 82–95, 23.6 and 17.8 years in the living trees are close to peaks at 87–94, 24.1 and 17.8 years detected in the subfossil chronology; Fig. 2a, b). In the low-frequency band of 80–254 years, the subfossil chronology shows a high concentration of variance (41.09%) but only 12.49% is reached in the modern chronology. Peaks at 47–51, 35, 23.6, 20.1 and 17.8 years are statistically significant in the modern chronology but do not exceed the *a priori* 95% confidence level in the Blackman-Tukey spectrum from the subfossil series. Association between the spectra of the living and subfossil records is also observed through a cross-spectra comparison in the frequency domain (Fig. 2c). The variances in the cross-amplitude spectra show relatively strong correspondence over the resolved frequency range equivalent to periods centred at 136–153, 81–94, 47–53, 35, 24, 17.8 years and other peaks over the higher-frequency range between 6.6 and 2.14 years (Fig. 2c inset). The broad correspondence between spectra suggest the possibility that similar processes have influenced the radial growth of both subfossil and modern *Fitzroya* trees.

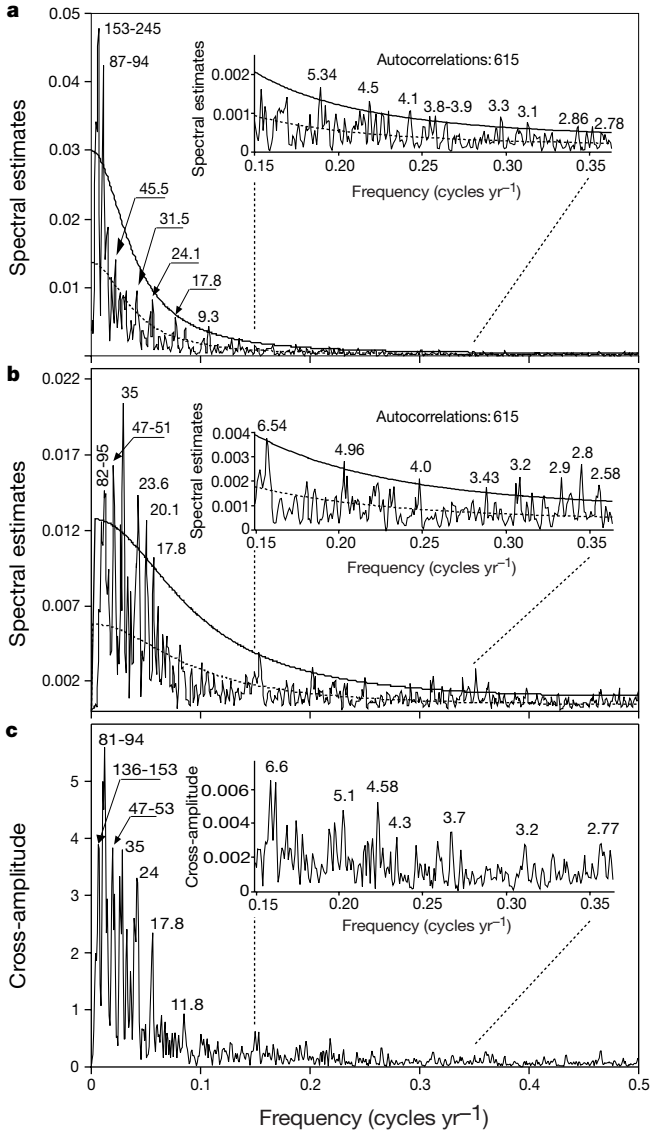

Figure 2 The spectral and cross-spectral characteristics of the subfossil (**a**) and living (**b**) *F. cupressoides* woods. We determined that 615 lags of the autocorrelation function (~50% the series length) were adequate to resolve the frequency spectrum with high resolution and moderate stability. The 95% confidence limits of the Blackman-Tukey[28] (BT) spectrum were estimated from a ''red noise'' null continuum based on the lag-1 autocorrelation coefficient. The periods are given in years for each individual peak. The (Hamming) bandwidth that we used was equal to 5. The maximum entropy[29] (ME) spectrum (not shown) was estimated from a 123-term prediction error filter (10% of the series length) using Burg's[30] algorithm. For comparison, the same analyses were performed for a similar time span (1,229-years) on a set of three millennium-long living *Fitzroya* chronologies (Lenca[11], Cisne[27] and Costa[31] chronologies, respectively) standardized in a similar way as the subfossil chronology. In this case we choose the amplitudes of the first eigenvector to develop our spectral estimates. The spectra are shown over the frequency range 0–0.50. **c**, The cross-spectral relationships between subfossil and modern chronologies. Expanded details of each power spectrum are shown in the insets.

Focusing on longer timescales, it is evident from the spectral density distribution that the ~150–250-year waveform is a characteristic of the Pelluco chronology, and may reflect low-frequency variations of climate during the late Pleistocene. Oscillations of the order of ~200 years have been found in late Pleistocene–Holocene records from marine cores from the west side of the Antarctic peninsula[22]. Solar modulation may be a possible forcing mechanism at this frequency because there is evidence of a near 220-year ^{14}C cycle as a result of sunspots[23]. Other cyclic fluctuations in the Pelluco chronology on a decadal to centennial timescale may also be attributed to varying solar activity. Atmospheric $\Delta^{14}C$ oscillations derived from tree-ring chronologies covering almost the entire Holocene (a 9,600-yr record)[23] show changes with periodicities close to 22 and 90 years, cycles related respectively to Hale and Gleissberg global solar changes. In a similar way, the oscillatory modes detected in the subfossil tree-ring chronology at the 87–94-year and the 24.1-year periods may correspond to periodicities related to both Hale and Gleissberg solar cycles contained in the 'modern' (Holocene) tree-ring records.

Determining the forcing mechanisms that produced the short-term cycles in our record is less straightforward. The El Niño/Southern Oscillation (ENSO) appears to be the largest single source of present-day global inter-annual climate variability. ENSO has operated for most of the Holocene, and strong climate shifts associated with El Niño events have been documented by, among other proxies, South American tree rings[4,12,13]. But for earlier times, data from marine cores imply that during glacial sea-level low-stands, the ocean/atmosphere conditions in the inter-tropical Pacific prevented or dramatically reduced the functioning of the ENSO system[24,25]. Furthermore, there are indications that the ENSO system probably operated during middle–late Pleistocene interglacials and warm interstadial periods, although overall climate and boundary conditions at these stages may have been too different to permit the characteristic ENSO climate variability in terms of frequency, intensity and recurrence[26]. Thus, some of the high-frequency oscillations at timescales of 2–7 years observed in our subfossil chronology still remain to be assessed in relation to other ancient high-resolution records.

F. cupressoides tree-rings are known to correlate well with summer temperatures[4,11,13]. This relationship permits reconstruction of Late Holocene climate fluctuations in the northern Patagonian Andes, at least during the past two millennia[4]. Uniformitarianism suggests that most of the tree-growth oscillations observed in our subfossil tree-ring Pelluco chronology may be attributed to summer temperature variability during Pleistocene interstadials at early stages of OIS 3. Hence, the oscillations of the order of 150–250 years detected in this chronology may have the same forcing as century-scale oscillations observed in temperature reconstructions of the Late

© 2001 Macmillan Magazines Ltd

Holocene derived from tree-ring data[4].

Our study suggests that comparable cycles in tree growth occurred between interstadials of the last glaciation and today, and hence that similar factors have affected the radial growth of *Fitzroya* since the Late Pleistocene. Considering that the Earth's atmosphere—and the ocean/atmosphere system—were significantly disturbed during the glacial cycles of the Late Pleistocene, the notable similarity in the spectral properties of the Pelluco subfossil and modern *F. cupressoides* chronologies suggests that the forcing mechanisms of climate during the interstadials have not changed dramatically. The potential for developing very long tree-ring chronologies—from the present day back several millennia—is one of the most promising results in southern South America dendrochronology[15,27]. Our Pelluco tree-ring chronology represents a high-resolution window that allows us the possibility of analysing fluctuations in tree growth and climate during warmer events of the last glacial stage in southern Chile, where other very old palaeorecords (>50,000 yr) are rare. □

Received 17 October 2000; accepted 18 January 2001.

1. Oldfield, F. (ed.) Global Change Report No. 45 (International Geosphere-Biosphere Programme (IGBP), Stockholm, 1998).
2. Fritts, H. C. *Reconstructing Large-Scale Climatic Patterns from Tree-Ring Data* (Univ. Arizona Press, Tucson, 1991).
3. Pilcher, J. R., Baillie, M. G. L., Schmidt, B. & Becker, B. A 7,272-year tree-ring chronology for western Europe. *Nature* **312,** 150–152 (1984).
4. Villalba, R. *et al.* in *Climate Fluctuations and Forcing Mechanisms of the Last 2,000 Years* (eds Jones, P. D., Bradley, R. S. & Jouzel, J.) 161–189 (Springer, Berlin, 1996).
5. Bradley, R. S. *Quaternary Paleoclimatology* (Chapman & Hall, London, 1992).
6. Clapperton, C. *Quaternary Geology and Geomorphology of South America* (Elsevier, Amsterdam, 1993).
7. Denton, G. H. *et al.* Geomorphology, stratigraphy, and radiocarbon chronology of Llanquihue Drift in the area of the southern Lake District, Seno Reloncaví, and Isla Grande de Chiloé, Chile. *Geografis. Ann. A* **81,** 167–229 (1999).
8. Heusser, C. J., Heusser, L. E. & Lowell, T. V. Paleoecology of the southern Chilean Lake District—Isla Grande de Chiloé during middle—late Llanquihue glaciation and deglaciation. *Geografis. Ann. A* **81,** 231–284 (1999).
9. Heusser, C. J. *et al.* Pollen sequence from the Chilean Lake District during the Llanquihue glaciation in marine oxygen Isotope Stages 4-2. *J. Quat. Sci.* **15,** 115–125 (2000).
10. Denton, G. H. *et al.* Interhemispheric linkage of paleoclimate during the last glaciation. *Geografis. Ann. A* **81,** 107–153 (1999).
11. Lara, A. & Villalba, R. A 3620-year temperature record from *Fitzroya cupressoides* tree rings in southern South America. *Science* **260,** 1104–1106 (1993).
12. Villalba, R. Tree-ring and glacial evidence for the Medieval Warm Epoch and the Little Ice Age in southern South America. *Clim. Change* **26,** 183–197 (1994).
13. Roig, F. A. Dendroklimatologische Untersuchungen an *Fitzroya cupressoides* im Gebiet der Küstenkordillere un der Südlichen Anden. Thesis, Basel Univ. (1996).
14. Miller, A. in *Climates of Central and South America* (ed. Schwerdtfeger, W.) 113–145 (Elsevier, Amsterdam, 1976).
15. Roig, F. A., Roig, C., Rabassa, J. & Boninsegna, J. A. Fuegian floating tree-ring chronologies from subfossil *Nothofagus* woods. *Holocene* **6,** 469–476 (1996).
16. Lomnitz, C. Major earthquakes and tsunamis in Chile during the period 1535 to 1965. *Geol. Rundsch.* **59,** 938–960 (1970).
17. Klohn, C. Beobachtungen über die Reste eines späteiszeitlichen Alerceswaldes. *Z. Naturfreunde Wanderer* **1975–1976,** 75–78 (1976).
18. Lara, A. The dynamics and disturbance regimes of *Fitzroya cupressoides* forests in the south-central Andes of Chile. Thesis, Univ. Colorado (1991).
19. Porter, S. C. Pleistocene glaciation in the southern Lake District of Chile. *Quat. Res.* **16,** 263–292 (1981).
20. Cook, E. R., Briffa, K. R., Shiyatov, S. G. & Mazepa, V. S. in *Methods of Dendrochronology* (eds Cook, E. R. & Kairiukstis, L. A.) 104–123 (Kluwer, Dordrecht, 1990).
21. Cook, E. R., Briffa, K. R., Meko, D. M., Graybill, D. A. & Funkhouser, G. The 'segment length curse' in long tree-ring chronology development for palaeoclimatic studies. *Holocene* **5,** 229–237 (1995).
22. Leventer, A. *et al.* Productivity cycles of 200–300 years in the Antarctic Peninsula region: Understanding linkages among the sun, atmosphere, oceans, sea ice, and biota. *Geol. Soc. Am. Bull.* **108,** 1626–1644 (1996).
23. Stuiver, M. & Braziunas, T. F. Atmospheric ^{14}C and century-scale solar oscillations. *Nature* **338,** 405–408 (1989).
24. Lammy, F., Hebbeln, D. & Wefer, G. Late Quaternary precessional cycles of terrigenous sediment input off the Norte Chico, Chile (27.5S) and palaeoclimatic implications. *Palaeogeogr. Palaeoclimatol. Palaeoecol.* **141,** 233–251 (1998).
25. Salinger, M. J. Palaeoclimates north and south. *Nature* **291,** 106–107 (1981).
26. Markgraf, V. *et al.* Evolution of late Pleistocene and Holocene climates in the circum-South Pacific land areas. *Clim. Dyn.* **6,** 193–211 (1992).
27. Boninsegna, J. A. in *Climate Since A. D. 1500* (eds Jones, P. D. & Bradley, R. S.) 446–462 (Routledge, London, 1992).
28. Jenkins, G. M. & Watts, D. G. *Spectral Analysis and its Applications* (Holden-Day, San Francisco, 1968).
29. Marple, S. L. Jr. *Digital Spectral Analysis with Applications* (Prentice Hall, Englewood Cliffs, New Jersey, 1987).
30. Burg, J. P. in *Modern Spectrum Analysis* (ed. Childers, D. G.) 42–48 (IEEE Press, New York, 1978).
31. Lara, A. *et al.* in *Dendrochronology in Latin America* (ed. Roig, F. A.) 217–244 (EDIUNC, Mendoza, 2000).

Acknowledgements

We thank J. Betancourt, D. Stahle, V. Markgraf and J. Pilcher for comments on the manuscript. AMS dates were provided in part through funding by NSF (Earth System History) and the Inter-American Institute (IAI).

Correspondence and requests for materials should be addressed to F.A.R. (email: froig@lab.cricyt.edu.ar).

Simulating the amplification of orbital forcing by ocean feedbacks in the last glaciation

M. Khodri, Y. Leclainche, G. Ramstein, P. Braconnot, O. Marti & E. Cortijo

LSCE, CE-Saclay, 91191, Gif sur Yvette, France

According to Milankovitch theory, the lower summer insolation at high latitudes about 115,000 years ago allowed winter snow to persist throughout summer, leading to ice-sheet build-up and glaciation[1]. But attempts to simulate the last glaciation using global atmospheric models have failed to produce this outcome when forced by insolation changes only[2–5]. These results point towards the importance of feedback effects—for example, through changes in vegetation or the ocean circulation—for the amplification of solar forcing[6–9]. Here we present a fully coupled ocean–atmosphere model of the last glaciation that produces a build-up of perennial snow cover at known locations of ice sheets during this period. We show that ocean feedbacks lead to a cooling of the high northern latitudes, along with an increase in atmospheric moisture transport from the Equator to the poles. These changes agree with available geological data[10–15] and, together, they lead to an increased delivery of snow to high northern latitudes. The mechanism we present explains the onset of glaciation—which would be amplified by changes in vegetation—in response to weak orbital forcing.

Previous simulations using atmosphere general circulation models have shown that the atmosphere alone is unable to produce perennial snow, which is required to start a glaciation[2–7,16]: several studies[3,16] related this failure to model resolution and snow parametrization. However, a major drawback of these simulations was that the ocean surface temperature and vegetation cover were prescribed to their modern values[2–9]. A previous study showed that biosphere–atmosphere interactions help to create favourable conditions for ice-sheet growth[9], but did not succeed in simulating perennial snow cover. For the period of the onset of the last glaciation, studies of planktonic and benthic foraminifera from the North Atlantic Ocean led to the conclusion that the meridional gradient of sea surface temperature (SST) was enhanced before glacial inception—with very cold SST at high latitudes[10] (a cooling of around 4 °C from present-day values) while low latitudes were slightly warmer[10,12] than at present. These studies[10,14,17–19] assumed that the changes in SST pattern were probably due to a shift of deep-water formation from the Norwegian Sea to the North Atlantic. Therefore changes in ocean circulation must have had a large effect on the high-latitude heat budget. These hypotheses remain untested by coupled ocean–atmosphere general circulation models. We tested this possible mechanism for glacial inception using the IPSL-CM2[20] ocean–atmosphere coupled model (see Methods section).

We performed a 100-year-long sensitivity experiment, called here the '115 kyr BP' run, which only differs from the 120-year control experiment in the Earth's orbital parameters, which are set for 115,000 years before present (BP)[21] (Table 1). The concentration of

© 2001 Macmillan Magazines Ltd